scientific reports

Check for updates

OPEN

ALKBH5 regulates etoposide-induced cellular senescence and osteogenic differentiation in osteoporosis through mediating the m^{6}A modification of VDAC3

Yansheng Huang[1], Sibo Wang[1], Dong Hu[2], Li Zhang[2] & Shaoyan Shi[2]✉

Osteoporosis, a common bone disease in older individuals, involves the progression influenced by N6-methyladenosine (m6A) modification. This study aimed to elucidate the effects of VDAC3 m6A modification on human bone mesenchymal stromal cell (BMSC) senescence and osteogenic differentiation. BMSCs were treated with etoposide to induce senescence. Senescence was assessed by β-galactosidase staining and quantitative real-time PCR (qPCR), and osteogenic differentiation was evaluated using Western blot, alkaline phosphatase, and alizarin red S staining. VDAC3 and ALKBH5 expression were quantified by qPCR, and their interaction was assessed by RNA immunoprecipitation (RIP) and luciferase reporter assay. m6A methylation was analyzed using the Me-RIP assay. VDAC3 expression was significantly decreased in etoposide-treated BMSCs (1.00 ± 0.13 vs. 0.26 ± 0.06). VDAC3 overexpression reduced etoposide-induced senescence and promoted osteogenic differentiation. ALKBH5 overexpression inhibited VDAC3 m6A modification (1.00 ± 0.095 vs. 0.233 ± 0.177) and its stability. ALKBH5 knockdown decreased etoposide-induced senescence and promoted osteogenic differentiation, effects that were reversed by VDAC3 knockdown. YTHDF1 was identified as the m6A methylation reader, and its overexpression inhibited VDAC3 stability. We demonstrated that ALKBH5 inhibited osteogenic differentiation of etoposide-induced senescent cells through the inhibition of VDAC3 m6A modification, and YTHDF1 acted as the m6A methylation reader. These findings provide a novel theoretical basis for the treatment of osteoporosis.

Keywords Osteoporosis, Osteogenic differentiation, m6A, VDAC3, ALKBH5

Osteoporosis is a systemic skeletal disorder characterized by low bone mass and deterioration of bone microarchitecture, leading to increased bone fragility and susceptibility to fractures[1]. Primary osteoporosis encompasses several subtypes, including postmenopausal osteoporosis (Type I), senile osteoporosis (Type II), and idiopathic osteoporosis (juvenile type)[2,3]. Among these, postmenopausal and senile osteoporosis are the most prevalent forms[2,3]. Osteoporotic fractures are among the primary causes of disability and mortality in elderly populations[4]. Consequently, the prevention and effective management of osteoporosis are crucial for improving the quality of life in older adults.

Cellular senescence is a key contributor to the pathogenesis of age-related osteoporosis. Osteoporosis primarily arises from disturbances in bone remodeling, which involves the balance between bone formation by osteoblasts and bone resorption by osteoclasts[5]. Bone mesenchymal stromal cells (BMSCs) play a critical role in bone remodeling. Senescent BMSCs tend to differentiate into adipocytes rather than osteoblasts, and their accumulation in bone tissue disrupts the osteogenic differentiation capacity of BMSCs with advancing age[6]. Inhibiting senescence to promote osteogenic differentiation has emerged as a novel therapeutic strategy for osteoporosis[7]. Reactive oxygen species (ROS) is considered cytotoxic and are predominantly generated by mitochondria[8]. Accumulating evidence suggests that the accumulation of ROS-induced damage contributes to the process of cellular senescence[9]. Voltage-dependent anion-selective channel 3 (VDAC3) is a potential sensor of mitochondrial ROS levels and is one of the isoforms of VDAC, a family of pore-forming proteins located

[1]Department of Spine Surgery, Honghui Hospital, Xi'an Jiaotong University, Xi'an 710000, Shaanxi, China. [2]Department of Hand Surgery, Honghui Hospital, Xi'an Jiaotong University, Xi'an 710000, Shaanxi, China. ✉email: shishaoyan0502@163.com

in the mitochondrial outer membrane[10]. VDAC3 cysteine over-oxidation is associated with ROS abundance in the mitochondrial intermembrane space and is considered a marker of aging[11]. The regulation of VDAC3 may therefore be significant for inhibiting cellular senescence. However, the involvement of VDAC3 in the progression of osteoporosis through mediating cellular senescence remains unclear.

RNA modifications are pervasive and essential for maintaining cellular homeostasis and function through dynamic regulation of gene expression[12]. Among these modifications, N6-methyladenosine (m6A) is the most prevalent modification of eukaryotic mRNAs[13]. m6A modification is a dynamic and reversible process regulated by methyltransferases and demethylases, playing crucial roles in various aspects of RNA biology, including splicing, translation, stability, localization, and higher-order structure formation[14–16]. Recent studies have demonstrated that m6A modification is involved in the pathogenesis of multiple diseases, such as cancer, cardiovascular diseases, and fatty liver diseases[17–19]. Specifically, m6A modification has been shown to mediate the progression of osteoporosis[20,21]. Therefore, targeting m6A modification holds promise for the treatment of osteoporosis. In this study, we investigated the effect of VDAC3 m6A modification on the regulation of osteogenic differentiation and cellular senescence in osteoporosis. The contributions of this study include:

1. The first investigation of the role of VDAC3 in osteogenic differentiation.
2. The elucidation of the regulatory effect of VDAC3 on osteoporosis induced by cellular senescence.
3. The exploration of the mechanism by which m6A modification regulates cellular senescence and osteogenic differentiation through modulating VDAC3 expression.

This study may provide novel insights and a potential therapeutic target for the treatment of osteoporosis.

Results

VDAC3 expression is decreased in etoposide-treated BMSCs

To investigate the role of cellular senescence in osteoporosis, we conducted a microarray analysis to identify differentially expressed genes (DEGs) in elderly patients with osteoporosis compared to middle-aged non-osteoporotic donors. The results are represented using a heatmap (Fig. 1A), showing multiple upregulated and downregulated genes in elderly osteoporotic patients relative to non-osteoporotic controls. KEGG pathway enrichment analysis was performed on the downregulated genes, revealing their enrichment in several signaling pathways, including those related to cellular senescence (Fig. 1B). VDAC3 was found to be enriched in the cellular senescence pathway, prompting us to focus on this gene for further study. We measured the expression of VDAC3 in etoposide-treated BMSCs and observed a significant decrease in VDAC3 expression upon etoposide treatment (Fig. 1C). These findings suggested that VDAC3 may serve as a potential target in the context of osteoporosis.

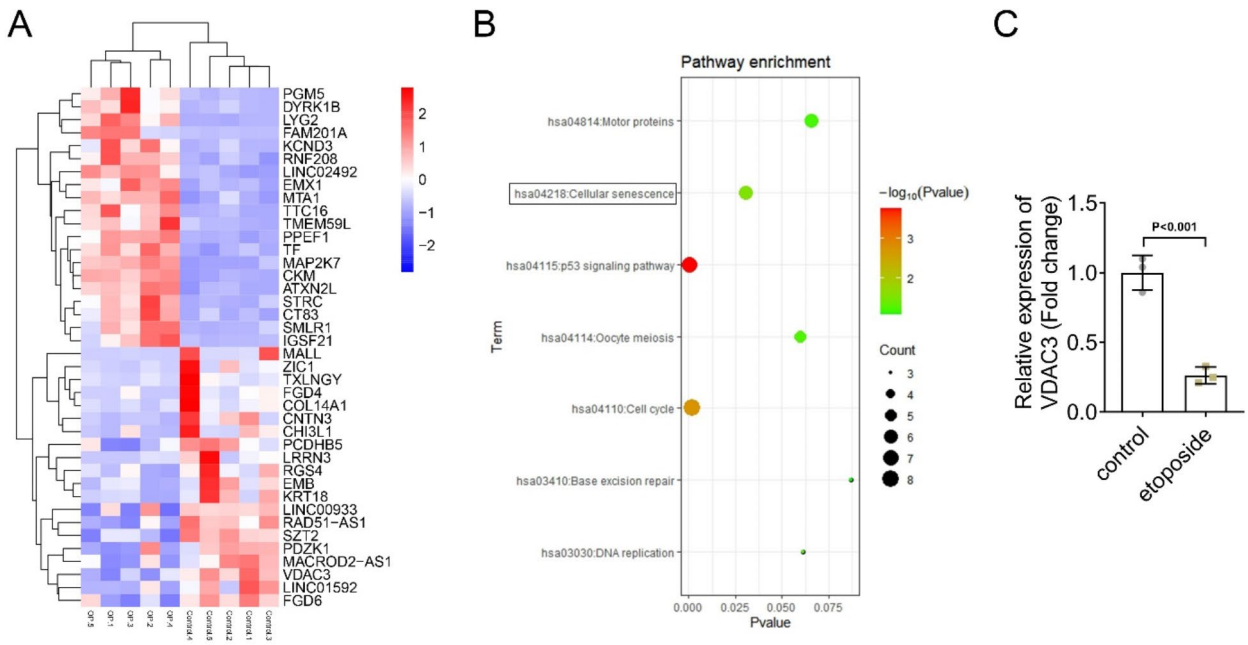

Fig. 1. VDAC3 expression was decreased in etoposide-induced BMSCs. (**A**) Differentially expressed genes in elderly patients with osteoporosis and non-osteoporotic donors were identified from the GSE35956 dataset. (**B**) DEGs enriched pathways were predicted by KEGG pathway enrichment analysis. (**C**) qPCR was performed to measure the expression of VDAC3 in BMSCs induced by 20 μM etoposide or not.

VDAC3 overexpression inhibits cellular senescence and promotes osteogenic differentiation in etoposide-treated BMSCs

To explore the functional role of VDAC3 in osteogenic differentiation, we transfected BMSCs with pcDNA3.1-VDAC3 plasmids, resulting in a marked increase in VDAC3 expression (Fig. 2A). Subsequently, we observed that etoposide treatment increased the number of senescent cells, whereas VDAC3 overexpression significantly reduced this number (Fig. 2B and C). We then examined the expression of aging markers and found that etoposide elevated the expression of p21 and p16, but VDAC3 overexpression partially reversed this elevation (Fig. 2D and E). Next, we induced osteogenic differentiation of BMSCs and found that etoposide treatment inhibited the expression of osteogenic differentiation-related proteins, including RUNX2, COL1A1, and ALP. However,

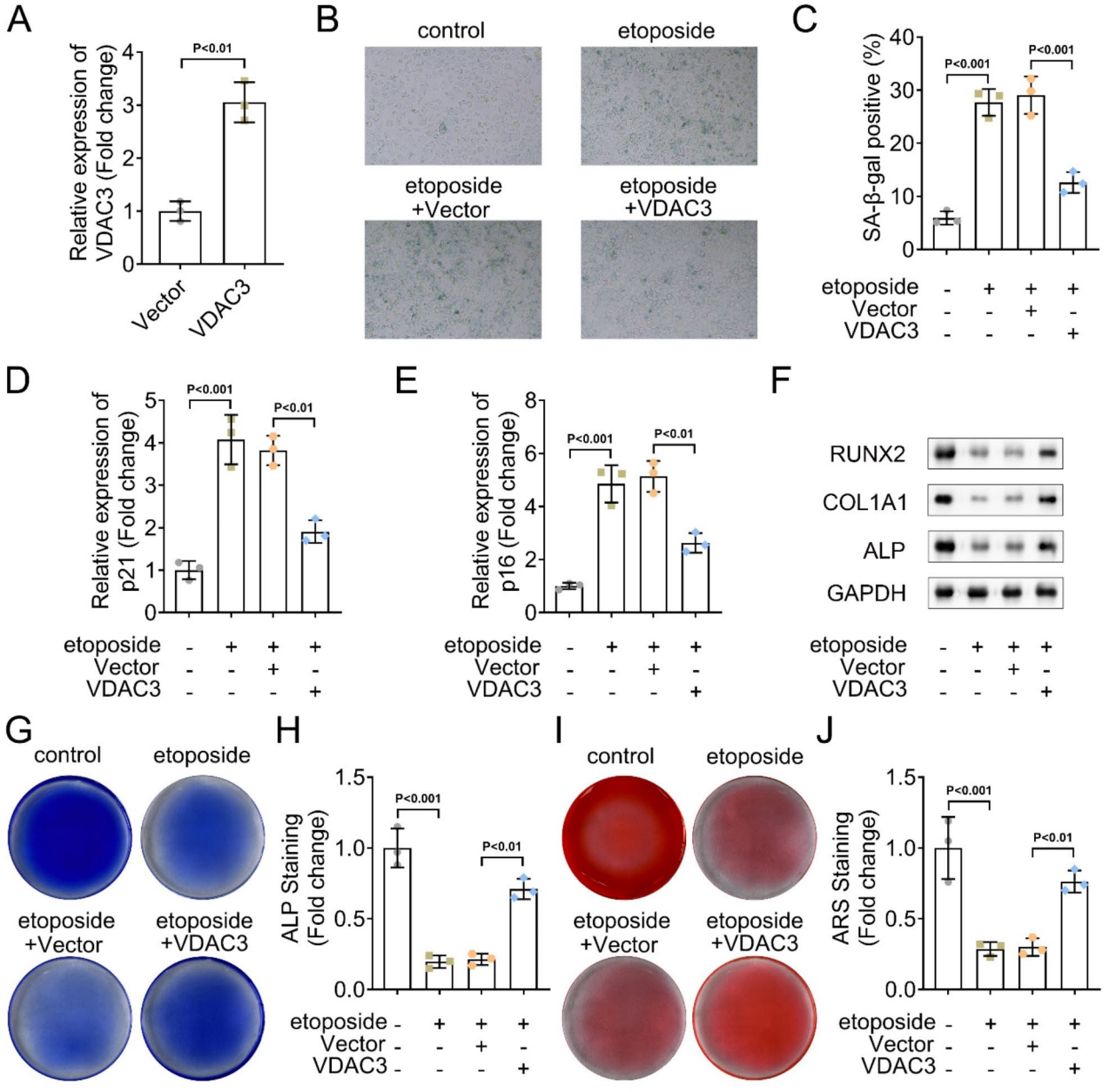

Fig. 2. Overexpression of VDAC3 inhibited cellular senescence and promoted osteogenic differentiation in etoposide-induced BMSCs. (**A**) qPCR was performed to measure the expression of VDAC3 in BMSCs following pcDNA3.1 and pcDNA3.1-VDAC3 transfection. (**B** and **C**) Cellular senescence was assessed using a senescence β-galactosidase staining kit and observed using a microscope. The expression of (**D**) p21 and (**E**) p16 in BMSCs was measured by qPCR. (**F**) The protein levels of RUNX2, COL1A1 and ALP were measured using western blot. (**G** and **H**) ALP staining was conducted using a BCIP/NBT alkaline phosphatase colour development kit after 14 d of osteogenic differentiation induction on BMSCs. (**I** and **J**) An ARS staining kit for osteogenesis was performed to ARS staining after 14 d of osteogenic differentiation induction on BMSCs.

these protein levels were upregulated by VDAC3 overexpression in etoposide-treated BMSCs (Fig. 2F). Alkaline phosphatase (ALP) staining and alizarin red S (ARS) staining further suggested that etoposide significantly inhibited ALP activity and calcium deposition, which were restored by VDAC3 overexpression (Fig. 2G-J). Collectively, these results indicated that VDAC3 overexpression inhibited cellular senescence and promotes osteogenic differentiation in etoposide-treated BMSCs.

ALKBH5 overexpression inhibits the m6A modification of VDAC3

To investigate the mechanism by which VDAC3 influences cellular senescence and osteogenic differentiation, we transfected BMSCs with pcDNA3.1-METTL3, pcDNA3.1-METTL14, pcDNA3.1-FTO, pcDNA3.1-WTAP, and pcDNA3.1-ALKBH5, observing elevated expression of these genes following transfection (Fig. 3A). We then determined VDAC3 expression in cells transfected with different plasmids using qPCR. The results showed that VDAC3 expression was significantly decreased by ALKBH5 overexpression (Fig. 3B). Moreover, the m6A modification level of VDAC3 was significantly reduced by ALKBH5 overexpression (Fig. 3C). The interaction between VDAC3 and ALKBH5 was confirmed by RNA immunoprecipitation (RIP) (Fig. 3D). Potential m6A modification sites in VDAC3 were predicted (Fig. 3E), and the top three sites are presented in Fig. 3F. A dual-luciferase reporter assay was performed to identify which site was indeed modified by m6A. The results suggested that ALKBH5 overexpression significantly reduced the luciferase activity of the wild-type site 3 (wt-site3, Fig. 3I), but did not affect the activity of the other two sites (Fig. 3G, H). Additionally, we demonstrated that ALKBH5 overexpression accelerated the degradation of VDAC3, indicating that ALKBH5 overexpression inhibited its stability (Fig. 3J). In conclusion, ALKBH5 overexpression inhibited the m6A modification of VDAC3 and its stability.

VDAC3 knockdown reverses the effect on cellular senescence and osteogenic differentiation in etoposide-induced BMSCs with ALKBH5 knockdown

To assess whether ALKBH5 affects VDAC3 to regulate cellular senescence and osteogenic differentiation, we performed rescue experiments. The expression of ALKBH5 and VDAC3 was significantly reduced following ALKBH5 and VDAC3 knockdown, respectively (Fig. 4A and B). ALKBH5 knockdown significantly suppressed cellular senescence in etoposide-treated BMSCs, an effect that was partially restored by VDAC3 knockdown (Fig. 4C and D). qPCR results showed that the expression of aging markers p21 and p16 was inhibited by ALKBH5 knockdown, whereas their expression was increased by VDAC3 knockdown following ALKBH5 downregulation (Fig. 4E and F). The protein levels of osteogenic differentiation-related markers RUNX2, COL1A1, and ALP were upregulated by ALKBH5 knockdown, but knockdown of VDAC3 partially inhibited their protein levels in sh-ALKBH5-transfected cells (Fig. 4G). Finally, ALP staining and ARS staining results suggested that ALKBH5 knockdown significantly increased ALP staining intensity and calcium deposition, indicating that ALKBH5 knockdown promoted osteogenic differentiation. This effect was reversed by VDAC3 knockdown (Fig. 4H-K). In conclusion, ALKBH5 knockdown inhibited cellular senescence and promoted osteogenic differentiation, effects that were reversed by VDAC3 knockdown.

YTHDF1 recognizes VDAC3 m6A modification

To identify the m^6A methylation reader of VDAC3, we transfected BMSCs with overexpression plasmids of YTHDF1, YTHDF2, YTHDF3, YTHDC1, YTHDC2, IGF2BP1, IGF2BP2, and IGF2BP3, and observed increased expression of these genes following transfection (Fig. 5A). Next, we measured the expression of VDAC3. The results showed that only YTHDF1 overexpression significantly increased the expression of VDAC3 (Fig. 5B). Moreover, YTHDF1 overexpression increased the luciferase activity of the wild-type VDAC3 (WT) construct, while the luciferase activity of the mutant (MUT) construct was not affected (Fig. 5C), indicating that YTHDF1 interacts with VDAC3. In addition, overexpression of YTHDF1 increased the stability of VDAC3 mRNA (Fig. 5D). In summary, these data demonstrated that YTHDF1 was the m6A methylation reader for VDAC3.

Discussion

In the present study, we demonstrated that VDAC3 overexpression inhibited cellular senescence and promoted osteogenic differentiation. Furthermore, we revealed for the first time that ALKBH5 inhibited osteogenic differentiation in osteoporosis by suppressing the m6A modification of VDAC3.

Osteoporosis is a metabolic bone disease characterized by bone loss and structural damage, conditions that are particularly prevalent in postmenopausal women and older men[22,23]. It is well-established that senile osteoporosis is closely linked to aging processes[24]. Farr et al.[25] reported that bone formation by osteoblasts is increased while bone marrow adipose tissue is reduced, suggesting a shift in BMSC differentiation from osteoblasts to adipocytes, a mechanism thought to underlie age-related bone loss. Senescence of BMSCs is known to affect osteogenic differentiation[26]. Wu et al.[27] demonstrated that ZFAS1 knockdown in BMSCs facilitates osteogenic differentiation and suppresses cellular senescence. Liu et al.[28] investigated the role of SIRT3 in combating BMSC senescence and improving osteoporosis through stabilizing heterochromatic and mitochondrial homeostasis. VDAC3, a putative sensor of mitochondrial ROS levels, has been shown to be upregulated in Korean red ginseng-treated rats, which helps protect against testicular aging[29]. Additionally, VDAC3 containing the VDAC1 N-terminus is capable of complementing the lack of the yeast porin in mitochondrial respiration and ROS modulation, thereby conferring anti-aging properties to cells[30].

Despite the established role of cellular senescence in osteoporosis, the specific mechanisms by which VDAC3 regulates osteogenic differentiation and cellular senescence in osteoporosis remain unclear. Our study represents the first investigation into the role of VDAC3 in cellular senescence and osteogenic differentiation. We demonstrated that VDAC3 expression was decreased in BMSCs treated with etoposide, a known inducer

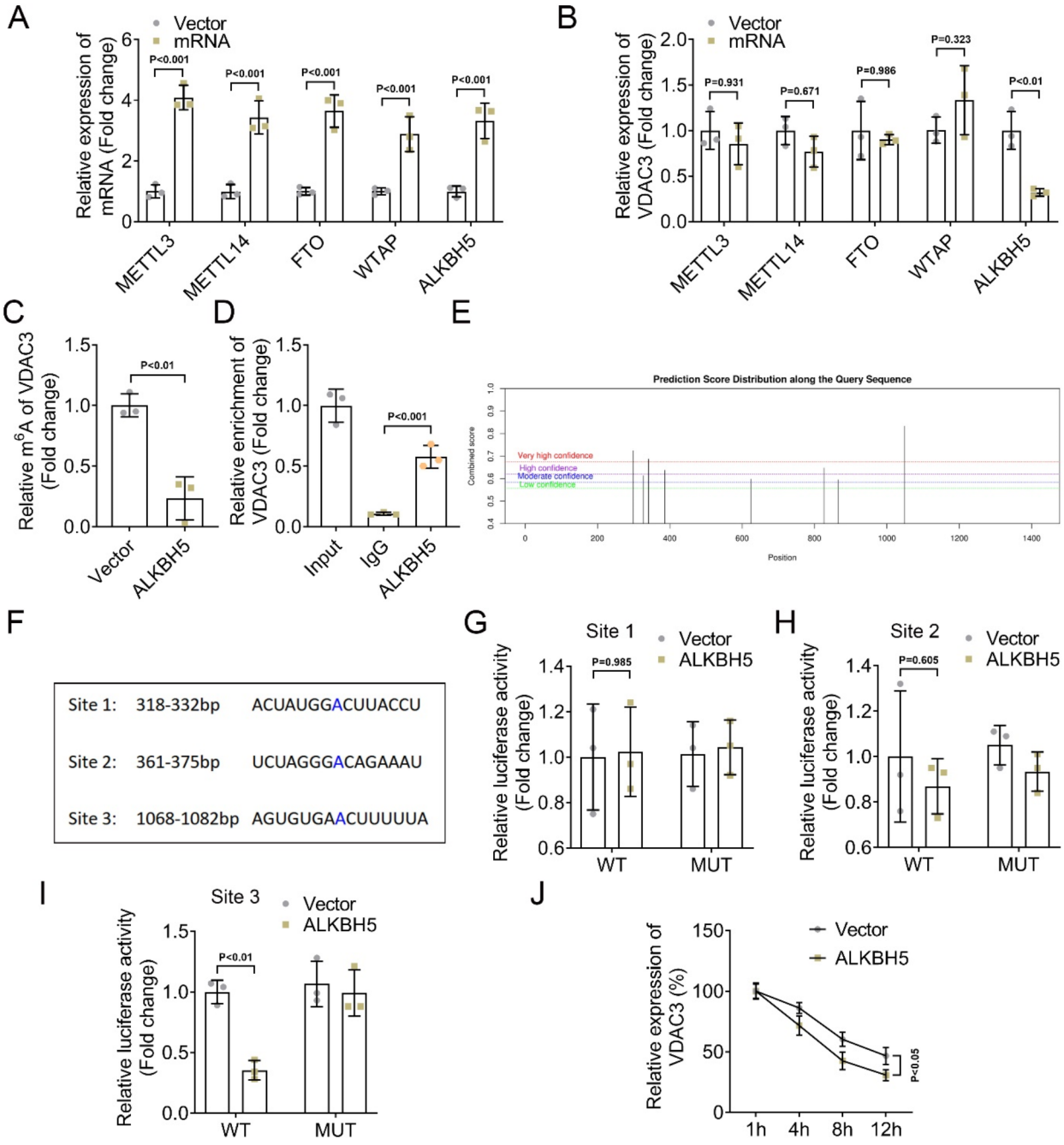

Fig. 3. ALKBH5 overexpression inhibited m6A modification of VDAC3. (**A**) The expression of METTL3, METTL14, FTO, WTAP and ALKBH5 in 293T cells following pcDNA3.1 and their respective overexpressing plasmids transfection was measured by qPCR. (**B**) The expression of VDAC3 in 293T cells transfected with pcDNA3.1-METTL3, pcDNA3.1-METTL14, pcDNA3.1-FTO, pcDNA3.1-WTAP and pcDNA3.1-ALKBH5 was measured by qPCR. (**C**) The m^6A level of VDAC3 in 293T cells transfected pcDNA3.1 or pcDNA3.1-ALKBH5 was assessed by MeRIP. (**D**) The enrichment of VDAC3 on ALKBH5 in 293T cells was determined by RIP. (**E**) The m6A sites were predicted using SRAMP database. (**F**) The top 3 potential sites in VDAC3. The luciferase activity of (**G**) wild type and mutant of site 1, (**H**) wild type and mutant of site 2 and (**I**) wild type and mutant of site 3 in 293T cells co-transfected with pcDNA3.1 or pcDNA3.1-ALKBH5 was measured by dual luciferase report. (**J**) qPCR was performed to evaluate VDAC3 expression in BMSCs transfected pcDNA3.1 or ALKBH5 overexpressing plasmids following treatment with 5 μg/mL actinomycin D for 1, 4, 8 and 12 h.

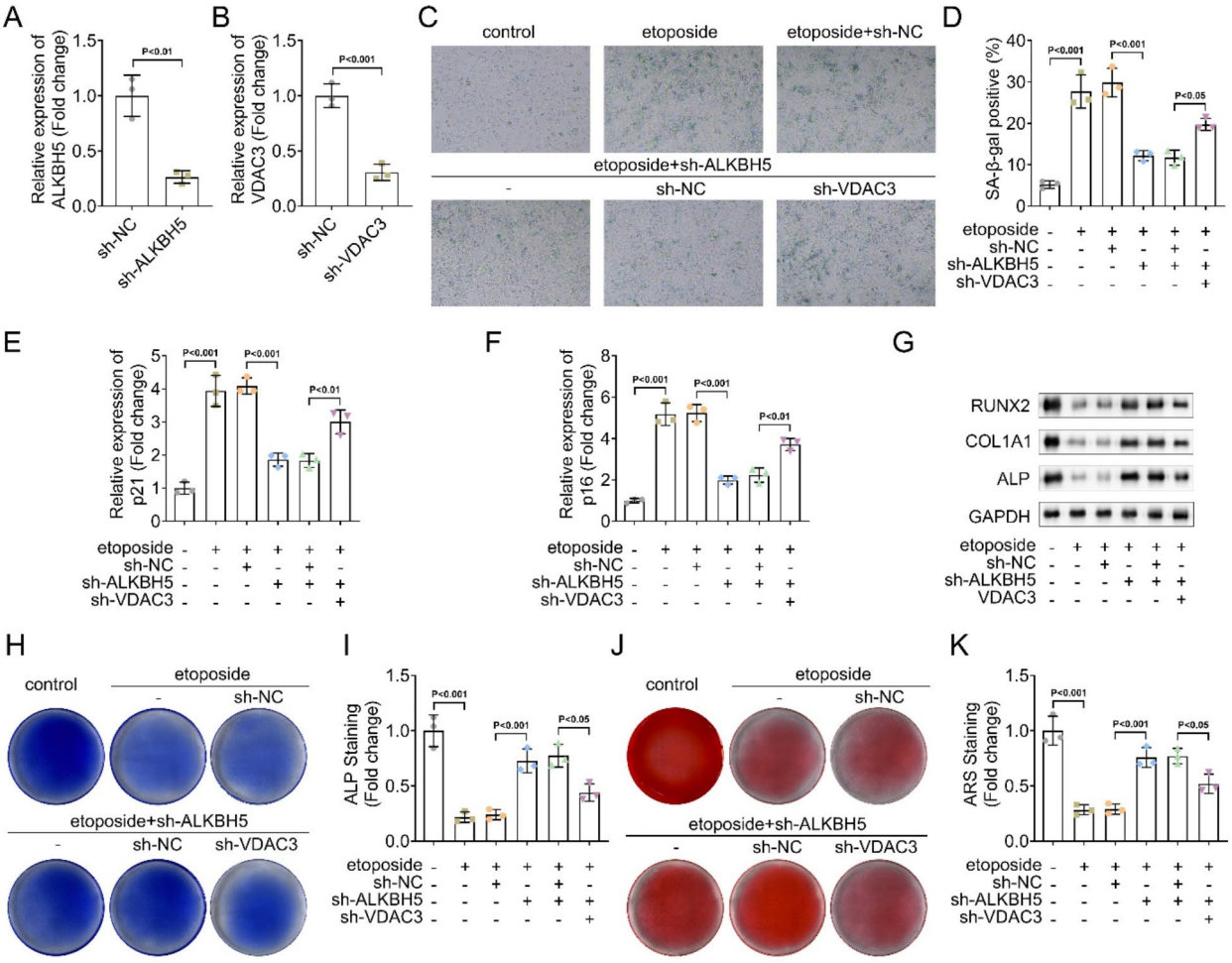

Fig. 4. VDAC3 knockdown reversed the effect on cellular senescence and osteogenic differentiation in etoposide-induced BMSCs with ALKBH5 knockdown. qPCR was performed to measure the expression of (**A**) ALKBH5 and (**B**) VDAC3 in BMSCs following sh-ALKBH5 and sh-VDAC3 transfection. (**C** and **D**) Cellular senescence of BMSCs was assessed using a senescence β-galactosidase staining kit. The expression of (**E**) p21 and (**F**) p16 in BMSCs transfected with different plasmids was measured by qPCR. (**G**) The protein levels of RUNX2, COL1A1 and ALP in BMSCs transfected with different plasmids were measured by western blot. (**H** and **I**) ALP staining was conducted using a BCIP/NBT alkaline phosphatase colour development kit after 14 d of osteogenic differentiation induction on BMSCs. (**J** and **K**) An ARS staining kit for osteogenesis was performed to ARS staining after 14 d of osteogenic differentiation induction on BMSCs.

of cellular senescence. Conversely, overexpression of VDAC3 reduced the number of senescent cells, inhibited the expression of aging markers p21 and p16, and promoted osteogenic differentiation in etoposide-induced BMSCs. These findings collectively suggested that upregulated VDAC3 inhibited cellular senescence and facilitates osteogenic differentiation, indicating that VDAC3 may be a key target for improving osteoporosis.

m6A modification has been shown to play a significant role in osteoporosis. Huang and Wang[20] demonstrated that knockdown of METTL14 suppresses osteogenesis of BMSCs and reduces bone mass in ovariectomized (OVX) mice by inhibiting m6A modification of SMAD1, thus destabilizing its expression. Furthermore, knockout of the m6A methyltransferase METTL3 in bone BMSCs induces pathological features of osteoporosis in mice[31]. In addition, METTL14 released by exosomes has been shown to increase the m6A methylation level of NFATc1, thereby inhibiting osteoclasts and helping postmenopausal osteoporosis patients maintain bone mass[32]. These findings collectively support the role of m6A modification in osteoporosis. However, the m6A modification on VDAC3 has not been previously reported. In our study, we confirmed that ALKBH5, an m6A demethylase, inhibited VDAC3 expression by decreasing m6A modification on VDAC3. ALKBH5 primarily performs post-transcriptional regulation of oncogenes or tumor suppressors in an m6A-dependent manner and plays a key role in various malignant tumors, including gastric cancer and colorectal cancer[33–35]. Nonetheless, the role of ALKBH5 in the development of osteoporosis remains unclear. In the current study, we confirmed that ALKBH5 knockdown inhibited cellular senescence and facilitates osteogenic differentiation in etoposide-treated BMSCs, while VDAC3 knockdown reversed these effects caused by ALKBH5 knockdown. These results

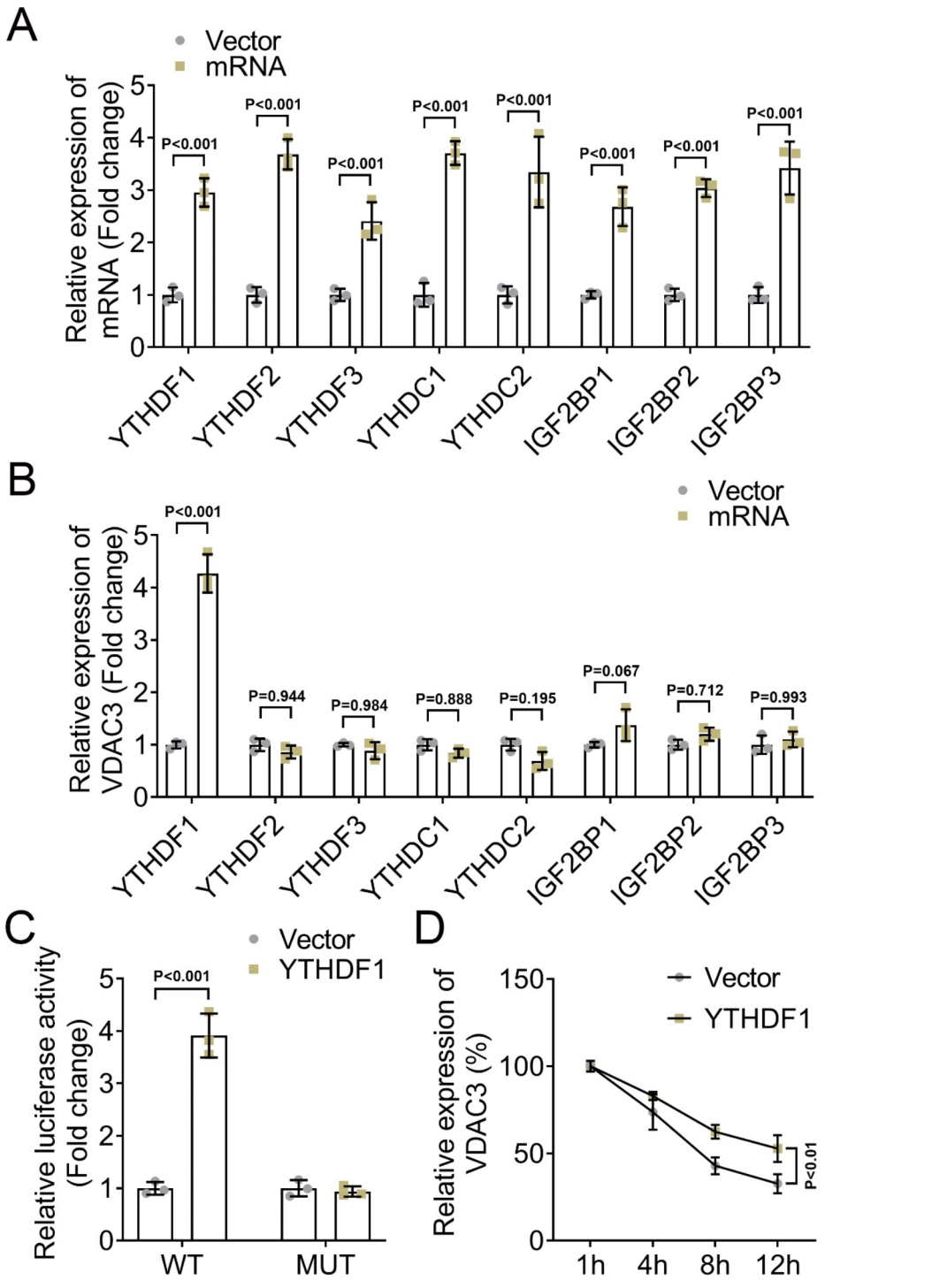

Fig. 5. YTHDF1 mediated the degradation of VDAC3 mRNA by m^{6}A modification. qPCR was performed to measure the expression of different m6A readers in BMSCs following transfection of pcDNA3.1 and their respective overexpressing plasmids. (**B**) The expression of VDAC3 in BMSCs transfected with pcDNA3.1 or different overexpressing plasmids was measured by qPCR. (**C**) The luciferase activity of VDAC3-wt and VDAC3-mut in 293T cells transfected with pcDNA3.1 or pcDNA3.1-YTHDF1 was measured by dual luciferase report. (**D**) qPCR was performed to evaluate VDAC3 expression in BMSCs following treatment with 5 μg/mL actinomycin D for 1, 4, 8 and 12 h.

indicated the negative regulatory effect of ALKBH5 on VDAC3 expression, cellular senescence, and osteogenic differentiation.

In addition, we identified YTHDF1 as the reader of VDAC3 m6A modification. m6A methylation reader proteins typically act as functional mediators that regulate the splicing, transport, stability, storage, and translation status of m6A-modified RNA[36]. YTHDF1 is a member of the m6A reader family and plays a critical role in the development of various cancers[37]. In recent years, Liu et al.[38] demonstrated that YTHDF1 promotes the osteogenic differentiation of BMSCs through translational control of ZNF8[39]. Shi et al.[39] showed that hypoxia suppresses osteogenic differentiation and increases the expression of YTHDF1, which translationally regulates its downstream factor thrombospondin-1 (THBS1) in an m6A-dependent manner, potentially counteracting hypoxia-induced osteogenic inhibition through the YTHDF1/THBS1 pathway. In our study, we first revealed that YTHDF1 overexpression promoted the mRNA stability of VDAC3, indicating that YTHDF1 recognizes VDAC3 m6A methylation during the regulation of cellular senescence and osteogenic differentiation.

Conclusion

In conclusion, this study provided the first evidence that ALKBH5 promoted cellular senescence and inhibited osteogenic differentiation in osteoporosis by suppressing the m6A modification of VDAC3. In conclusion, this study provides the first evidence that ALKBH5 promotes cellular senescence and inhibits osteogenic differentiation in osteoporosis by suppressing the m6A modification of VDAC3. These findings may offer a novel therapeutic target and approach for the treatment of osteoporosis. However, the study is subject to certain limitations. Specifically, no animal experiments were conducted, and the expression and function of VDAC3 were not verified in vivo. These aspects will be addressed in future work to further validate the role of VDAC3 in osteoporosis and explore its underlying mechanisms.

Methods

Cell culture and treatment

Human BMSCs and 293T cells were obtained from Procell (Wuhan, China). The cells were cultured in Dulbecco's Modified Eagle Medium (DMEM; Gibco, Grand Island, NY, USA) supplemented with 10% fetal bovine serum (FBS; Gibco) and maintained in a humidified incubator at 37 °C with 5% CO_2. To induce cellular senescence, BMSCs were treated with 20 μM etoposide for 48 h and then maintained in fresh medium for 4 days. For the induction of osteogenic differentiation, BMSCs were cultured in α-minimum essential medium (α-MEM; Gibco) supplemented with 10% FBS, 50 μg/mL ascorbic acid, 10 mM β-glycerol phosphate, and 0.1 μM dexamethasone for 14 days.

Cell transfection.

Cells in the logarithmic growth phase were inoculated in six-well plates (2×10^5 cells/well). The cells were transfected with short hairpin RNA targeting VDAC3 (sh-VDAC3), short hairpin RNA targeting ALKBH5 (sh-ALKBH5), a shRNA negative control (shNC), or overexpressing plasmids for VDAC3, METTL3, METTL14, FTO, WTAP, ALKBH5, YTHDF1, YTHDF2, YTHDF3, YTHDC1, YTHDC2, IGF2BP1, IGF2BP2, and IGF2BP3, along with an empty vector (pcDNA3.1) (GenePharma, Shanghai, China) using Lipofectamine 2000 (Invitrogen, Carlsbad, CA, USA) according to the manufacturer's instructions. The transfected cells were harvested 48 h post-transfection.

Bioinformatic analysis

The GSE35956 dataset was acquired from the Gene Expression Omnibus database (GEO, https://www.ncbi.nlm.nih.gov/geo/query/acc.cgi?acc=GSE35956). Data were analyzed using GEO2R. The DEGs were defined as $P < 0.05$ and a log (fold change) > 2. The downregulated genes were subjected to Kyoto Encyclopedia of Genes and Genomes (KEGG) enrichment analysis to predict enriched pathways. A p-value < 0.05 was considered the threshold for enrichment.

The m^6A sites in VDAC3 were predicted using the SRAMP database (http://www.cuilab.cn/sramp).

Quantitative real-time PCR (qPCR)

Total RNA was extracted from the cells using TRIzol reagent (Invitrogen, Carlsbad, CA, USA) according to the manufacturer's instructions. RNA purity was assessed by measuring the absorbance ratio at 260 nm to 280 nm (A260/A280), and RNA integrity was evaluated using agarose gel electrophoresis. Complementary DNA (cDNA) was synthesized from total RNA using a First Strand cDNA Synthesis Kit (Takara, Shiga, Japan). qPCR was performed using SYBR Green Master Mix (Thermo Fisher Scientific, Waltham, MA, USA) on a real-time PCR system. Relative mRNA expression was calculated using the $2^{-\Delta\Delta Ct}$ method as normalized to β-actin. The primers for qPCR are presented in Table 1.

Cellular senescence detection

Cellular senescence was detected using a Senescence β-Galactosidase Staining Kit (Beyotime, Beijing, China) according to the manufacturer's protocol. Briefly, BMSCs were fixed with 1 mL of β-galactosidase fixation solution for 15 min at room temperature, followed by overnight incubation with 1 mL of staining solution at 37 °C. After staining, the cells were observed under an optical microscope.

Western blot assay

Total protein was extracted from the cells using radio immunoprecipitation assay (RIPA) lysis buffer (Thermo Scientific, Waltham, MA, USA) and quantified using a BCA Protein Assay Kit (Beyotime, Beijing, China). Equal amounts of protein were separated by 10% SDS-PAGE and transferred onto PVDF membranes. The membranes

Gene	Forward Primer	Reverse Primer
CCNB2	CCGACGGTGTCCAGTGATTT	TGTTGTTTTGGTGGGTTGAACT
CCNB1	TCGCATCAAACTCTCTGGCTA	TGAGCGACTAAACTCACCACT
CCNE2	TCAAGACGAAGTAGCCGTTTAC	TGACATCCTGGGTAGTTTTCCTC
CDK1	AAACTACAGGTCAAGTGGTAGCC	TCCTGCATAAGCACATCCTGA
VDAC3	TTGTACCGAACACAGGAAAGAAG	CCCAGCCATAGATGGTTGGTC
FOXM1	CGTCGGCCACTGATTCTCAAA	GGCAGGGGATCTCTTAGGTTC
METTL3	TTGTCTCCAACCTTCCGTAGT	CCAGATCAGAGAGGTGGTGTAG
METTL14	AGTGCCGACAGCATTGGTG	GGAGCAGAGGTATCATAGGAAGC
FTO	ACTTGGCTCCCTTATCTGACC	TGTGCAGTGTGAGAAAGGCTT
WTAP	CTTCCCAAGAAGGTTCGATTGA	TCAGACTCTCTTAGGCCAGTTAC
ALKBH5	CGGCGAAGGCTACACTTACG	CCACCAGCTTTTGGATCACCA
YTHDF1	ACCTGTCCAGCTATTACCCG	TGGTGAGGTATGGAATCGGAG
YTHDF2	AGCCCCACTTCCTACCAGATG	TGAGAACTGTTATTTCCCCATGC
YTHDF3	TCAGAGTAACAGCTATCCACCA	GGTTGTCAGATATGGCATAGGCT
YTHDC1	AACTGGTTTCTAAGCCACTGAGC	GGAGGCACTACTTGATAGACGA
YTHDC2	AGGACATTCGCATTGATGAGG	CTCTGGTCCCCGTATCGGA
IGF2BP1	GCGGCCAGTTCTTGGTCAA	TTGGGCACCGAATGTTCAATC
IGF2BP2	AGTGGAATTGCATGGGAAAATCA	CAACGGCGGTTTCTGTGTC
IGF2BP3	TATATCGGAAACCTCAGCGAGA	GGACCGAGTGCTCAACTTCT

Table 1. The primers for qPCR.

were blocked with 5% skim milk for 1 h at room temperature and then incubated overnight at 4 °C with the following primary antibodies: anti-RUNX2 (1:1000, ab236639), anti-COL1A1 (1:1000, ab138492), anti-ALP (1:1000, ab307726), and anti-GAPDH (1:10,000, ab181602) (Abcam, Cambridge, UK). After washing with Tris buffer-Tween (TBST), the membranes were incubated with a secondary antibody (1:10,000, ab205718, Abcam) for 2 h at room temperature. Protein bands were visualized using an enhanced chemiluminescence (ECL) reagent (Yeasen Biotech, Shanghai, China) and imaged using an optical luminescence instrument.

Alkaline phosphatase (ALP) staining

The osteogenic differentiation of BMSCs was assessed using a BCIP/NBT Alkaline Phosphatase Color Development Kit (Beyotime, Beijing, China) according to the manufacturer's instructions. Briefly, the cells were fixed in 4% paraformaldehyde for 20 min and subsequently stained with the working solution for 30 min in the dark. Following staining, the cells were rinsed with distilled water and imaged.

Alizarin red S (ARS) staining

The osteogenic differentiation potential of BMSCs was also evaluated using an Alizarin Red S Staining Kit for Osteogenesis (Beyotime, Beijing, China) following the manufacturer's protocol. The cells were fixed in the provided fixing solution for 20 min, stained with Alizarin Red S solution for 30 min, and then imaged.

Methylated RNA immunoprecipitation (MeRIP)

The level of m6A modification on VDAC3 was quantified using a Magna MeRIP m6A kit (Merck, Darmstadt, Germany) according to the manufacturer's protocol. Briefly, 12 μg of anti-m6A antibody was pre-incubated with 50 μL of magnetic beads in IP buffer (150 mM NaCl, 0.1% NP-40, 10 mM Tris-HCl, pH 7.4) at room temperature for 1 h. Fragmented RNA (6 μg) was then added to the antibody-bead mixture and incubated at 4 °C for 4 h on a rotator. Following adequate washing with IP buffer, the mixture was treated with proteinase K to digest the proteins, and the bound RNAs were extracted using the phenol-chloroform method. The expression of VDAC3 was quantified by qPCR.

RNA immunoprecipitation (RIP)

RIP assays were performed using an Imprint RNA Immunoprecipitation Kit (Sigma-Aldrich, St. Louis, MO, USA) according to the manufacturer's instructions. Briefly, 293T cells were lysed in RIP lysis buffer containing protease and RNase inhibitors. To assess the interaction between VDAC3 and ALKBH5, the lysate was incubated overnight at 4 °C with magnetic protein A/G beads coated with either anti-ALKBH5 or anti-IgG (isotype control). After purification, RNA was isolated using TRIzol reagent, and the expression of VDAC3 was detected by qPCR.

Dual luciferase reports assay

Wild-type (wt)-VDAC3 and mutant (mut)-VDAC3 sequences containing putative ALKBH5 or YTHDF1 binding sites were cloned into the pGL3 vector to construct luciferase reporter plasmids. 293T cells were seeded in 96-well plates and co-transfected with the pcDNA3.1, pcDNA3.1-ALKBH5, or pcDNA3.1-YTHDF1 plasmids using Lipofectamine 2000 reagent for 24 h. Luciferase activity was measured using a Dual-Luciferase Reporter Assay System (Promega, Madison, WI, USA).

RNA stability assay
To determine the stability of VDAC3 mRNA, BMSCs were treated with 5 μg/mL actinomycin D (Merck, Darmstadt, Germany). mRNA expression was quantified by qPCR at 1, 4, 8, and 12 h post-treatment.

Statistical analysis
All statistical analyses were performed using SPSS 22.0 software. Data are presented as mean ± standard deviation based on at least three independent experiments. Comparisons between two or more groups were conducted using Student's t-test or one-way analysis of variance (ANOVA), respectively. Statistical significance was set at $P < 0.05$.

Data availability
The datasets used and/or analyzed during the current study are available from the corresponding author on reasonable request.

Received: 9 May 2024; Accepted: 1 October 2024
Published online: 08 October 2024

References
1. Armas, L. A. G. & Recker, R. R. Pathophysiology of osteoporosis: new mechanistic insights. *ENDOCRIN METAB. CLIN.* **41**, 475 (2012).
2. Lane, J. M., Russell, L. & Khan, S. N. Osteoporosis. *Clin. Orthop. Relat. Res.* **372**, 139 (2000).
3. Arceo-Mendoza, R. M. & Camacho, P. M. Postmenopausal osteoporosis: latest guidelines. *ENDOCRIN METAB. CLIN.* **50**, 167 (2021).
4. Vandenput, L. et al. Update of the fracture risk prediction tool FRAX: a systematic review of potential cohorts and analysis plan. *Osteoporos. Int.* **33**, 2103 (2022).
5. Gao, Y., Patil, S. & Jia, J. The development of Molecular Biology of osteoporosis. *INT. J. MOL. SCI.* **22**, 8182 (2021).
6. Kučuk, N., Primožič, M., Knez, Ž. & Leitgeb, M. Exosomes Engineering and their roles as Therapy Delivery Tools, therapeutic targets, and biomarkers. *INT. J. MOL. SCI.* **22**, 9543 (2021).
7. Khosla, S., Farr, J. N. & Kirkland, J. L. Inhibiting Cellular Senescence: a New Therapeutic paradigm for age-related osteoporosis. *J. Clin. Endocrinol. Metab.* **103**, 1282 (2018).
8. Balaban, R. S., Nemoto, S. & Finkel, T. Mitochondria, oxidants, and aging. *CELL* 120 483 (2005).
9. Liochev, S. I. Reactive oxygen species and the free radical theory of aging. *FREE RADICAL BIO MED.* **60**, 1 (2013).
10. Reina, S. et al. Voltage dependent Anion Channel 3 (VDAC3) protects mitochondria from oxidative stress. *REDOX BIOL.* **51**, 102264 (2022).
11. Reina, S., Guarino, F., Magri, A. & De Pinto, V. VDAC3 as a potential marker of mitochondrial status is involved in Cancer and Pathology. *FRONT. ONCOL.* **6**, 264 (2016).
12. Han, D. & Xu, M. M. RNA modification in the Immune System. *ANNU. REV. IMMUNOL.* **41**, 73 (2023).
13. Wiener, D. & Schwartz, S. The epitranscriptome beyond m 6 A. *Nat. Rev. Genet.* **22**, 119 (2021).
14. Wang, T., Kong, S., Tao, M. & Ju, S. The potential role of RNA N6-methyladenosine in Cancer progression. *MOL. CANCER.* **19**, 88 (2020).
15. Jiang, X. et al. The role of m6A modification in the biological functions and diseases. *Signal. Transduct. Target. Ther.* **6**, 74 (2021).
16. Deng, L. J. et al. m6A modification: recent advances, anticancer targeted drug discovery and beyond. *MOL. CANCER.* **21**, 52 (2022).
17. Wang, C. et al. RNA modification in cardiovascular disease: implications for therapeutic interventions. *Signal. Transduct. Target. Ther.* **8**, 412 (2023).
18. Yang, Y. et al. Dysregulated m6A modification promotes lipogenesis and development of non-alcoholic fatty liver disease and hepatocellular carcinoma. *MOL. THER.* **30**, 2342 (2022).
19. Lin, H., Wang, Y., Wang, P., Long, F. & Wang, T. Mutual regulation between N6-methyladenosine (m6A) modification and circular RNAs in cancer: impacts on therapeutic resistance. *MOL. CANCER.* **21**, 1 (2022).
20. Huang, C. & Wang, Y. Downregulation of METTL14 improves postmenopausal osteoporosis via IGF2BP1 dependent posttranscriptional silencing of SMAD1. *CELL. DEATH DIS.* **13**, 919 (2022).
21. You, Y. et al. WTAP-mediated m(6)a modification modulates bone marrow mesenchymal stem cells differentiation potential and osteoporosis. *CELL. DEATH DIS.* **14**, 33 (2023).
22. Srivastava, M. & Deal, C. Osteoporosis in elderly: prevention and treatment. *CLIN. GERIATR. MED.* **18**, 529 (2002).
23. Gosset, A., Pouillès, J. & Trémollieres, F. Menopausal hormone therapy for the management of osteoporosis. *BEST PRACT. RES. CL. EN.* **35**, 101551 (2021).
24. Pignolo, R. J., Law, S. F. & Chandra, A. Bone aging, Cellular Senescence, and osteoporosis. *JBMR Plus.* **5**, e10488 (2021).
25. Farr, J. N. et al. Targeting cellular senescence prevents age-related bone loss in mice. *NAT. MED.* **23**, 1072 (2017).
26. Hu, M. et al. NAP1L2 drives mesenchymal stem cell senescence and suppresses osteogenic differentiation. *AGING CELL.* **21**, e13551 (2022).
27. Wu, J. et al. Long noncoding RNA ZFAS1 suppresses osteogenic differentiation of bone marrow-derived mesenchymal stem cells by upregulating mir-499-EPHA5 axis. *MOL. CELL. ENDOCRINOL.* **539**, 111490 (2022).
28. Liu, F. et al. S-sulfhydration of SIRT3 combats BMSC senescence and ameliorates osteoporosis via stabilizing heterochromatic and mitochondrial homeostasis. *PHARMACOL. RES.* **192**, 106788 (2023).
29. Kim, I. H. et al. Korean Red Ginseng Up-regulates C21-Steroid hormone metabolism via Cyp11a1 gene in senescent rat testes. *J. GINSENG RES.* **35**, 272 (2011).
30. Reina, S. et al. Swapping of the N-terminus of VDAC1 with VDAC3 restores full activity of the channel and confers anti-aging features to the cell. *FEBS LETT.* **584**, 2837 (2010).
31. Wu, Y. et al. Mettl3-mediated m(6)a RNA methylation regulates the fate of bone marrow mesenchymal stem cells and osteoporosis. *NAT. COMMUN.* **9**, 4772 (2018).
32. Yang, J. G. et al. Exosome-targeted delivery of METTL14 regulates NFATc1 m6A methylation levels to correct osteoclast-induced bone resorption. *CELL. DEATH DIS.* **14**, 738 (2023).
33. Qu, J. et al. RNA demethylase ALKBH5 in cancer: from mechanisms to therapeutic potential. *J. HEMATOL. ONCOL.* **15**, 8 (2022).
34. Hu, Y. et al. Demethylase ALKBH5 suppresses invasion of gastric cancer via PKMYT1 m6A modification. *MOL. CANCER.* **21**, 34 (2022).
35. Zhai, J. et al. ALKBH5 Drives Immune Suppression Via Targeting AXIN2 to Promote Colorectal Cancer and Is a Target for Boosting Immunotherapy. *GASTROENTEROLOGY* 165 445 (2023).

36. Tan, X., Zheng, C., Zhuang, Y., Jin, P. & Wang, F. The m6A reader PRRC2A is essential for meiosis I completion during spermatogenesis. *NAT. COMMUN.* **14**, 1636 (2023).
37. Ren, W. et al. The function and clinical implication of YTHDF1 in the human system development and cancer. *Biomark. Res.* **11**, 5 (2023).
38. Liu, T. et al. The m6A reader YTHDF1 promotes osteogenesis of bone marrow mesenchymal stem cells through translational control of ZNF839. *CELL. DEATH DIS.* **12**, 1078 (2021).
39. Shi, D. et al. Yth m(6)a RNA-Binding protein 1 regulates Osteogenesis of MC3T3-E1 cells under Hypoxia via Translational Control of Thrombospondin-1. *INT. J. MOL. SCI.* **24**, 1741 (2023).

Author contributions
SS conceived the study; YH conducted the experiments; SW, DH and LZ analyzed the data; YH was a major contributor in writing the manuscript. All authors read and approved the final manuscript.

Funding
This study was supported by Natural Science Foundation of Shaanxi Province, Grant/Award Number: 2021SF-241.

Declarations

Competing interests
The authors declare no competing interests.

Additional information
Supplementary Information The online version contains supplementary material available at https://doi.org/10.1038/s41598-024-75033-9.

Correspondence and requests for materials should be addressed to S.S.

Reprints and permissions information is available at www.nature.com/reprints.

Publisher's note Springer Nature remains neutral with regard to jurisdictional claims in published maps and institutional affiliations.